

True parameters of ${}^4_{\Sigma}\text{He}$ hypernucleus

V.M.Kolybasov *

Lebedev Physical Institute, 117924 Moscow, Russia

Abstract

It is shown that the true parameters of ${}^4_{\Sigma}\text{He}$ differ from the observed ones. The reason is that the amplitude of ${}^4_{\Sigma}\text{He}$ production in the reaction ${}^4\text{He}(\text{K}^-, \pi^-)$ sharply varies just in the corresponding mass region. It leads to the small, but noticeable shift of the binding energy and the width. Besides, the data at the threshold of Σ^0 production is found to give an additional evidence that ${}^4_{\Sigma}\text{He}$ width cannot exceed $8.0 \div 8.5$ MeV.

PACS: 25.80.Nv, 21.80.+a, 24.10.-i, 24.50.+g

*e-mail: kolybasv@sci.lebedev.ru

The recent study of the missing mass spectrum from the reaction



at 600 MeV/c has revealed a peak in the region close to Σ production [1]. The peak corresponds to the bound ${}^4_\Sigma\text{He}$ state with parameters $E_{ex} = -7$ MeV and $\Gamma = 7$ MeV (E_{ex} is the missing mass to a pion measured from the sum of masses $\Sigma^0 + {}^3\text{He}$). Here we give the central values of the parameters, obtained in Ref. [1] with the help of several simple versions of the background approximation.¹

A production of ${}^4_\Sigma\text{He}$ actually realizes the unique case when the amplitude of resonance production is sharply varying function of mass just in the region of resonance mass. If the amplitude strongly changes on the resonance width, it can lead to the appreciable shift of the observed energy and width compared with the true values. As will be shown below, the amplitude of ${}^4_\Sigma\text{He}$ production in the process (1) rapidly varies in the E_{ex} interval from -10 MeV to 0, that is, just in the region of ${}^4_\Sigma\text{He}$ mass.

The missing mass spectrum from the reaction



was also studied in Ref. [1]. A comparison of the data on channels (1) and (2) shows the following. Almost all events of the reaction (1) are situated at $E_{ex} > 0$. They form a broad maximum which is usually associated with a quasifree Σ^- production [2]. In contrast to this, the channel (2) has also many events in the E_{ex} region from -40 to -10 MeV. They are obviously due to the tail of Λ production. Besides, the channel (2) has an enhancement at E_{ex} near zero, and a distinct peak at $E_{ex} = -7$ MeV corresponding to the bound ${}^4_\Sigma\text{He}$ state (see the histogram in Fig. 1). In what follows, primary attention will be focused on the region of the resonance peak. However at first it is necessary to discuss a physical nature of the “background”, that is the tail of Λ production and the region of “quasifree” Σ production. An

¹The threshold of $(\Sigma^- + t)$ channel is situated 2.6 MeV lower than the threshold of $(\Sigma^0 + {}^3\text{He})$ channel. So $E_{ex} = -7$ MeV corresponds to the binding energy 4.4 MeV.

attempt to describe E_{ex} spectrum from -40 to -20 MeV in terms of quasifree Λ production was unsuccessful. The corresponding curve decreased too rapidly in obvious contradiction with the data. The model of quasifree Λ production with subsequent rescattering on residual nuclear system therefore was applied. ${}^4\text{He}$ wave function in oscillator potential was used, and the oscillator parameter p_0 was considered as fitting one. Small values of p_0 result in too rapidly decreasing curve. For large p_0 values the curve, on the contrary, falls down too slowly, that contradicts the data at E_{ex} in the region $30 \div 50$ MeV. The optimum value is $p_0 = 150$ MeV/c which leads to the curve in Fig. 1. Certainly, such procedure is rather rough, and the corresponding errors will be considered later on.

As to the region $E_{ex} > 0$, the simplest mechanisms are quasifree Σ production which can be accompanied by Σ rescattering on residual nuclear system or by $\Sigma \rightarrow \Lambda$ conversion. The analysis of (K^-, π^\pm) reactions on ${}^9\text{Be}$, ${}^{12}\text{C}$ and ${}^4\text{He}$ was performed in Ref. [3]. It shows that the quasifree production gives a peak which is narrower and leftward shifted compared with the experimental one. At the same time an account of elastic and inelastic rescatterings together with the interference of corresponding amplitudes results in a good description of E_{ex} spectra. Thus, it is possible to suppose that the origin of a main part of the Fig. 1 spectrum in general is clear. It allows to study the region of ${}^4_\Sigma\text{He}$ peak and $E_{ex} \sim 0$ in more detail.

The most probable mechanism of ${}^4_\Sigma\text{He}$ production is presented in Fig. 2 (a) and (b). At first, Σ -hyperon is born on one of neutrons, and then it coalesce with residual nuclear system. The difference between Fig. 2 (a) and (b) is that in the first case we have the two-particle intermediate state ${}^3\text{He} - \Sigma^0$, and in the second case the three-particle state $p - d - \Sigma^0$ is present (there could also be four-particle state $p - p - n - \Sigma^0$). An amplitude of Fig. 2 (a) has singularities of two kinds: the root threshold singularity at $E_{ex} = 0$, and the triangle logarithmic singularity located in complex plane. The latter is also situated near $E_{ex} = 0$ for kinematical conditions of Ref. [1]. Modulus squared of the triangle graph amplitude M_Δ for this case is shown (without Breit-Wigner factor) by solid curve in Fig. 3. Here and further

we use the oscillator wave function of ${}^4\text{He}$ with the parameter $p_0 = 90 \text{ MeV}/c$ which gives the best description of ${}^4\text{He}(e, ep)$ data at small spectator momenta [4]. According to the evaluation of Ref. [1], the bound state of ${}^4_\Sigma\text{He}$ is located at $E_{ex} = -7 \text{ MeV}$ and has the width about 7 MeV. Figure 3 shows that $|M_\Delta|^2$ strongly varies on the resonance width. It can noticeably influence the result of ${}^4_\Sigma\text{He}$ parameters estimation from the experimental data.

It is worth noting that such sharp behavior of the amplitude is well known for the case of stopped kaon capture $K^-d \rightarrow p\Lambda\pi^-$. The pion spectrum for this reaction has a distinct peak [5] associated with the triangle graph with the conversion $\Sigma \rightarrow \Lambda$ (see Ref. [6]). A cusp behavior was also indicated in Ref. [7] devoted to stopped K^- capture in ${}^4\text{He}$. A possibility of the distortion for Breit–Wigner form in the case of nearthreshold resonance was also mentioned in Ref. [8].

Sharp behavior of $|M_\Delta|^2$ is characteristic only for the triangle graph of Fig. 2 (a) with a two–particle intermediate state. The graph of Fig. 2 (b) with a three–particle intermediate state leads to the smooth amplitude whose maximum is shifted rightward (see also Ref. [9]). It is shown by dotted curve in Fig. 3. Therefore the comparative contribution of Fig. 2 (a) and (b) graphs is rather important. It is determined by the relations of the left lower and upper vertices of both graphs. As to the nuclear vertices, their relation can be obtained from the available data on ${}^4\text{He}(e, ep)$ reaction [4]. They show that the vertex of two–particle ${}^4\text{He}$ decay is much more than the vertices of three and four–particle decays at relative momenta up to 250 MeV/c. There are no direct information on the vertices of virtual ${}^4_\Sigma\text{He}$ decays. Owing to a lack of data on sigma–nuclear interactions, the reliable evaluations are now hardly possible. However, we have no reasons to assume that the two–particle channel is preferred here. Therefore it is possible to assert only that the contribution of Fig. 2 (a) graph in any case should be noticeable against a “background” of Fig. 2 (b) graph. It is indirectly confirmed also by the results of Ref. [7].

There is one more interesting point originating during the analysis of the data. Modulus squared of Fig. 2 (a) graph is the product of the modulus squared of triangle graph with

constant lower vertex, which is shown by solid line in Fig. 3, and Breit–Wigner resonance factor. It is easy to see that this product has two peaks. The first corresponds to the resonance, and the second is located at $E_{ex} \approx 0$. A ratio of these peaks depends on the width of the resonance. For the case of narrow resonance, the “cusp” maximum near $E_{ex} = 0$ will be suppressed by Breit–Wigner factor, and for the case of broad resonance this maximum will be large. It imposes additional constraints on the resonance width. The point is that, though the data have an enhancement near $E_{ex} = 0$, it is not large. Moreover, a ratio of magnitudes of indicated maxima in total result [with account for Fig. 2 (b)] is sensitive to the relative contribution of Fig. 2 (a) and (b) graphs. The relative magnitude of the maximum at $E_{ex} = 0$ decreases with increasing a partial yield of continuum [Fig. 2 (b)] in the intermediate state. This fact appears to be rather important for fitting the data.

A rapid variation of the ${}^4_{\Sigma}\text{He}$ production amplitude as function of E_{ex} was not taken into account in the analysis of Ref. 1. It made the procedure not quite correct. Let’s look what are the results of the correct account for the production mechanism, corresponding to the graphs of Fig. 2 (a) and (b). We shall begin from attempt to describe E_{ex} spectrum with the parameters from Ref. [1], that is, the binding energy 4.4 MeV (it corresponds to $E_{ex} = -7$ MeV) and the width 7 MeV. The best description for this case is shown in Fig. 4 (a). It is necessary to accept here that the ratio of Fig. 4 (a) and (b) contributions is not more than 1:5. Otherwise there would be too large enhancement at $E_{ex} = 0$ in obvious contradiction with the data.² It is possible to see that the peak is described not so well, especially the left wing.

The situation can be improved by a modification of ${}^4_{\Sigma}\text{He}$ parameters. Various versions of the fitting procedure have shown that the best description of E_{ex} spectrum could be obtained with the binding energy 5.4 MeV (it corresponds to $E_{ex} = -8$ MeV) and the width 8 MeV. This fit is shown in Fig. 4 (b). The smaller width would lead to a poor description

²We mean the ratio without account of Breit–Wigner resonance factor. The contribution of Fig. 2 (b) graph to actual spectrum remains small as the resonance factor hardly suppresses the whole area $E_{ex} > 10$ MeV.

for the left wing of the resonance peak. The larger width would lead to too strong peak at $E_{ex} = 0$. The latter is also essential in another respect. As indicated above, the technique for inclusion of Λ production tail is incomplete. If the solid curve in Fig. 1 were more rapidly decreasing, then, after its subtraction, the resonance left wing would be broader. It would demand the larger value of the width. However, as it appears, the width more than $8.0 \div 8.5$ MeV is forbidden as it would too strengthen the peak near $E_{ex} = 0$. Besides, to keep the magnitude of this peak in reasonable limits, it is necessary to suppose that the contribution of multi-particle intermediate states in Fig. 2 is several times more than the contribution of two-particle states. From here follows that the probabilities of virtual ${}^4_{\Sigma}\text{He}$ decays to three and four-particle channels are much larger than to two-particle ones.

In summary we shall mark the following:

1. The amplitude of ${}^4_{\Sigma}\text{He}$ production was shown to be a sharply varying function of mass just in the resonance region.
2. It results in a small, but noticeable shift of ${}^4_{\Sigma}\text{He}$ parameters in comparison with the results of Ref. [1]. The central values of both the binding energy and the width are increased on 1 MeV. This shift, though is not large and does not exceed the limits of the errors indicated in Ref. [1], nevertheless can be important for estimations of Σ -nuclear interaction [10].
3. From the comparison of the cross section near $E_{ex} = 0$ with calculations, the additional evidence is obtained that ${}^4_{\Sigma}\text{He}$ width does not exceed $8.0 \div 8.5$ MeV. The indication is also obtained on preferred role of multiparticle channels for virtual ${}^4_{\Sigma}\text{He}$ decay.
4. The considered case can be of interest in more general aspect as the unique example of a resonance on a sharply varying background.
5. The appearance of more statistically based data will require to refine the calculations in several points: (a) using a realistic ${}^4\text{He}$ wave function; (b) account of a form factor in the vertex of the resonance production in Fig. 2 (a); (c) elaboration of a reliable model for the Λ production tail in (K^-, π^-) processes.

Acknowledgments: The author is indebted to O. D. Dalkarov and T. E. O. Ericson for

discussions. He also appreciate the hospitality of The Svedberg Laboratory of the Uppsala University where a part of this investigation was done.

References

- [1] T. Nagae *et al.*, Phys. Rev. Lett. **80**, 1605 (1998).
- [2] C. B. Dover, D. J. Millener, A. Gal, Phys. Rep. **184**, 1 (1989).
- [3] O. D. Dalkarov and V. M. Kolybasov, e-print nucl-th/9901040.
- [4] J. M. Laget, Nucl. Phys. **A497**, 391c (1989); J. F. J. van den Brandt *et al.*, Phys. Rev. Lett. **60**, 2006 (1988); Nucl. Phys. **A534**, 637 (1991); J. M. Le Goff *et al.*, Phys. Rev. C **50**, 2278 (1994).
- [5] T. H. Tan, Phys. Rev. Lett. **23**, 395 (1969).
- [6] R. H. Dalitz, *Strange particles and strong interactions* (Oxford University Press, 1962); A. E. Kudryavtsev, JETP Letters **14**, 137 (1971); G. Torek, A. Gal, and J. M. Eisenberg, Nucl. Phys. **A362**, 405 (1981).
- [7] R. H. Dalitz and A. Deloff, Nucl. Phys. **A585**, 303c (1995).
- [8] T. Harada and Y. Akaishi, Progr. Theor. Phys. **96**, 145 (1996).
- [9] R. H. Dalitz and A. Deloff, Nucl. Phys. **A547**, 181c (1992).
- [10] T. Harada, S. Shinmura, Y. Akaishi, and H. Tanaka, Nucl. Phys. **A507**, 715 (1990).

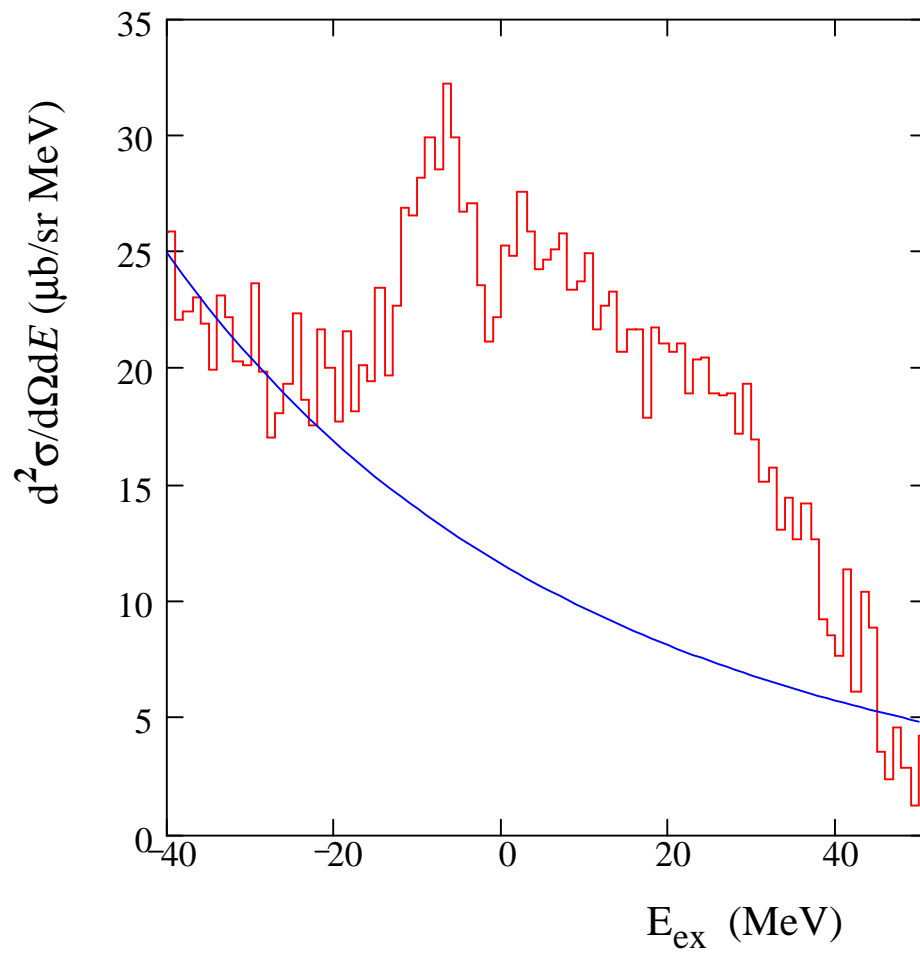
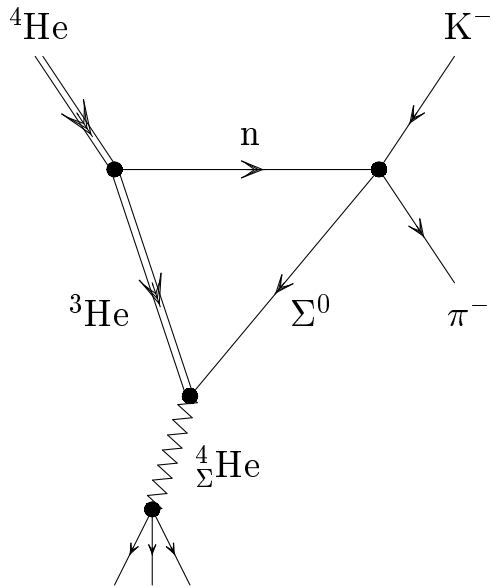
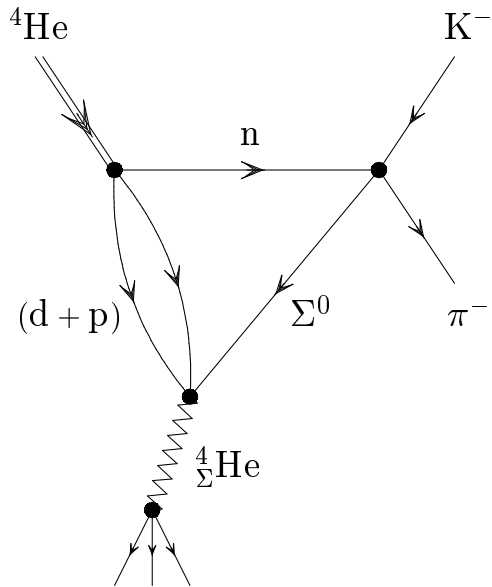


Figure 1: The data of Ref. [1] on the differential cross sections of the reaction ${}^4\text{He}(\text{K}^-, \pi^-)$. The solid curve is the approximation of the tail of direct Λ production.



a



b

Figure 2: Graphs for ${}^4_{\Sigma}\text{He}$ production in the reaction ${}^4\text{He}(\text{K}^-, \pi^-)$.

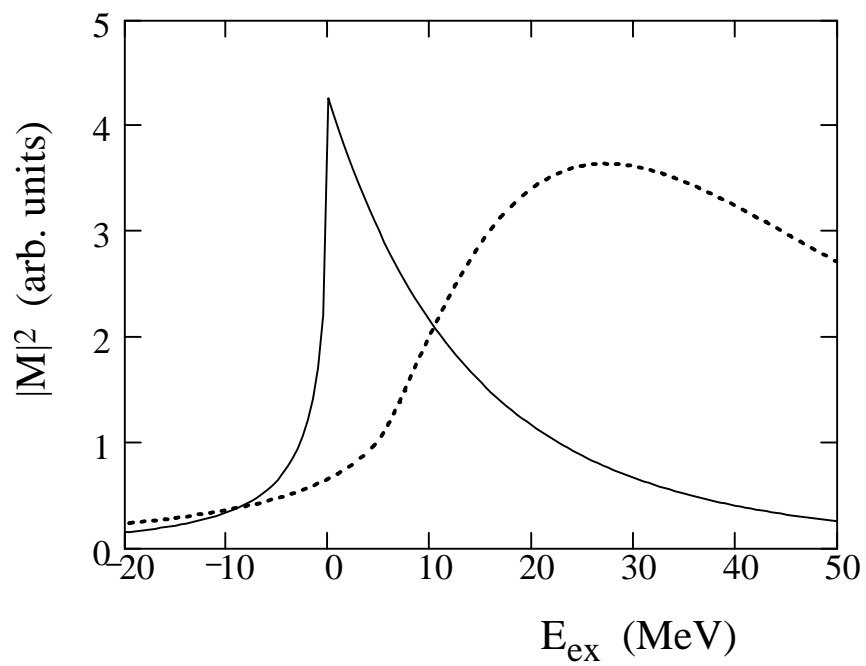


Figure 3: $|M_{\Delta}|^2$ for the triangle graphs of Fig. 2 with two-particle (solid curve) and three-particle (dotted curve) intermediate states.

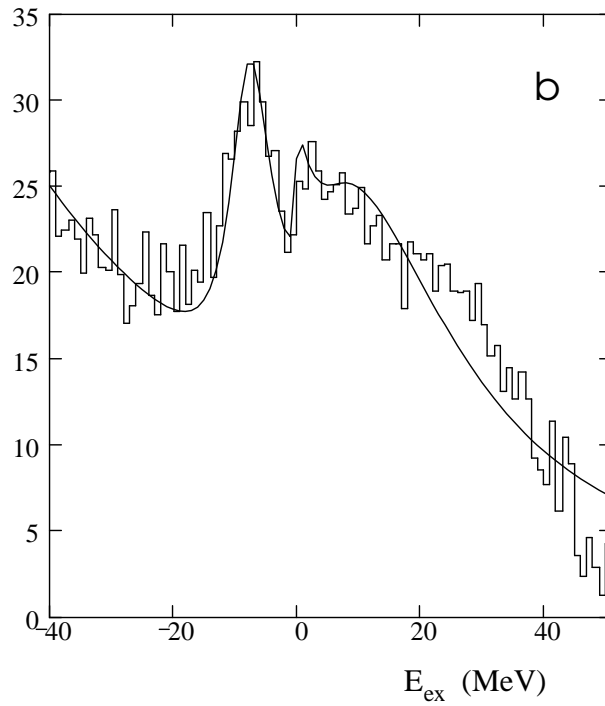
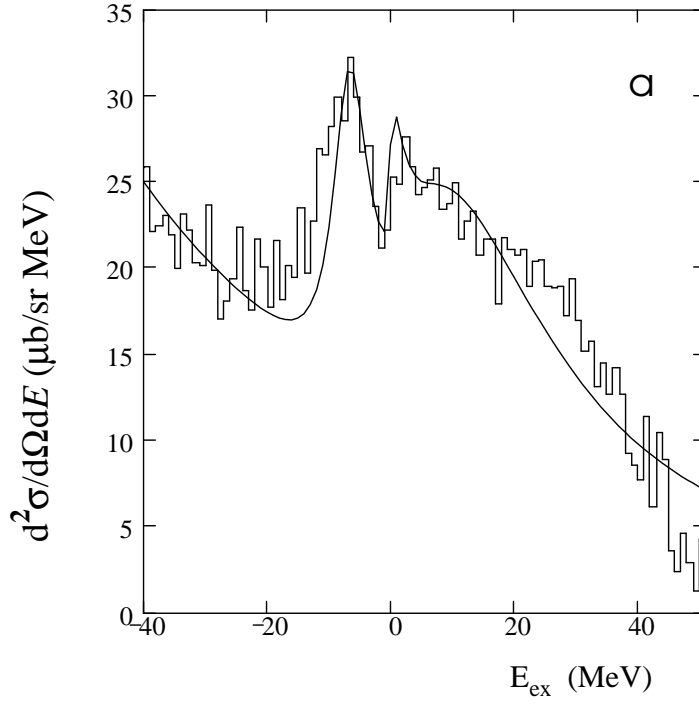


Figure 4: Theoretical description of E_{ex} spectrum for the reaction ${}^4\text{He}(K^-, \pi^-)$: (a) with ${}^4\text{He}$ parameters from Ref. [1]; (b) with the binding energy 5.4 MeV and the width 8 MeV.